

Pairwise correlations in large two-dimensional Cu–O clusters: a new nonlocal path integral Monte Carlo algorithm

V. A. Kashurnikov

Moscow Engineering Physics Institute, 115409 Moscow, Russia

(Submitted 19 May 1995)

Zh. Éksp. Teor. Fiz **108**, 1796–1809 (November 1995)

A new nonlocal path integral Monte Carlo algorithm for a CuO_2 plane is proposed. The technique is based on breaking the CuO_2 plane into five-site CuO_4 cells and converges rapidly. It can be used in studies of the semiconducting state symmetry. Pairwise correlation functions are calculated by incorporating additional time slices into the Monte Carlo scheme. To the best of our knowledge, characteristics of a Cu–O two-dimensional cluster with the number of atoms $N_a=768$ (16×16 CuO_2 cells) have been calculated for the first time. It was found that in given ranges of Emery's Hamiltonian parameters ($U_d=6t$, $\varepsilon=1-3t$, $U_p=V=0$), temperature ($T \geq 0.125t$), and carrier concentration ($0.7 \leq x \leq 1.5$) a) no off-diagonal long-range order, corresponding to the superconducting state, was detected in any coupling channel in the thermodynamic limit, and b) there is a tendency to divergence in both s^* and $d_{x^2-y^2}$ channels as the temperature decreases, but a more detailed analysis indicates that antiferromagnetic ordering is the main contributor to this effect. The typical correlation length equals three lattice constants and is close to the typical antiferromagnetic length. © 1995 American Institute of Physics.

1. INTRODUCTION

Recently the discussion of the high- T_c superconductivity mechanism has been concentrated on the symmetry of the order parameter (i.e., the symmetry of the wave function of the superconducting state).^{1,2}

A solution of this problem might yield additional information about the nature of the electron-electron interaction and formation of Cooper pairs, and the number of plausible theoretical models would be reduced considerably.³⁻⁵

The symmetry of the superconducting state cannot be unambiguously derived from available experimental data. In particular, measurements of gap anisotropy in Josephson functions and SQUIDS,⁶⁻¹¹ data on nuclear magnetic resonance,¹² Raman scattering,¹³ and scanning tunneling microscopy¹⁴ favor $d_{x^2-y^2}$ symmetry, whereas other experimental results such as measurements of angle-dependent photoemission¹⁵ and Josephson weak coupling¹⁶ indicate that the symmetry is s -type.

Note that in most experiments⁶⁻¹⁴ strong anisotropy of the order parameter was detected, but nodes of the order parameter as a function of the wave vector direction do not prove that its symmetry is d -type because the order parameter can also be zero when s -coupling is strongly anisotropic (s^*).^{2,3} In order to detect d -symmetry, one should measure the phase of the order parameter.² In this connection, measurements of NMR,¹² tunneling spectroscopy,⁸ and temperature dependence of the magnetic field penetration depth¹⁷ may contain more information.

Nonetheless, experimental data can be often interpreted in terms of both s^* -wave coupling and a combination of s^* - and $d_{x^2-y^2}$ -wave coupling.^{17,18}

The small coherence length, weak isotopic effect, and other anomalous properties of high- T_c superconductors have stimulated investigations of plausible nonphonon mecha-

nisms of superconductivity. In this regard, the most faithful HTS models are the Hubbard¹⁹ and Emery²⁰ models. However, analytic calculations using these models are fraught with considerable difficulty.^{21,22}

In this situation numerical methods are of great importance. They include exact diagonalization^{23,24} and Monte Carlo²⁵⁻²⁷ simulations, in which system parameters can be calculated without simplifying the model Hamiltonian, prescribing in advance the shape of the ground state wave function, or using rough approximations.

Exact diagonalization has been applied to Cu–O clusters described by the Emery model to calculate the binding energy of doping carriers and their correlation functions²⁸⁻³⁵ at $T=0$. It is found that carriers tend to pair up over a wide range of model parameters. As for pairwise symmetry, the calculation of pairwise correlations in a Cu_4O_8 cluster by the exact diagonalization method within the Emery model for s -, s^* - and $d_{x^2-y^2}$ -wave pairing³⁶ indicate that s^* -symmetry predominates. In the $t-J$ model, the diagonalization method indicates that d -symmetry prevails.³⁷

But the basic limitation of this method, namely the smallness of the analyzed system, makes it impossible to conclude unambiguously whether any one of the coupling modes can produce a superconducting state because, in order to settle the matter, one must ensure that pairwise correlations in the momentum space diverge in the thermodynamic limit.

Therefore quantum Monte Carlo techniques,^{25,27} which can be used to calculate thermodynamic averages of large clusters ($N_a=100-200$), must be employed in calculating system parameters versus cluster dimensions. These techniques, however, are flawed because they are not applicable at low temperatures ($T \sim 100$ K) owing to large statistical errors. Nonetheless, by using data obtained at temperatures at which the Monte Carlo is appropriate, there is some hope

of obtaining information about pairwise correlations and susceptibilities at lower temperatures, because strong correlation effects responsible for the superconducting phase transition can be detected through fluctuations at a temperature higher than that of the phase transition.²⁷

Now let us briefly review the investigations of the coupling symmetry using Monte Carlo techniques.

In the single-band, two-dimensional Hubbard model, a divergence was detected for the s -coupling³⁸ at any filling of the electron band. On the other hand, no s -coupling was found in the case of repulsion in the two-dimensional Hubbard model³⁹ since the correlation functions did not diverge in the limit $N_a \rightarrow \infty$. A similar result was obtained by Scalettar *et al.*⁴⁰ In the Emery model, the scaling analysis of pairwise correlations revealed a lack of off-diagonal long-range order in the s -channel in the thermodynamic limit.²⁷

In addition, many other papers about the Monte Carlo techniques have been published.⁴¹⁻⁴⁶ Unfortunately, they do not systematically analyze size effects on pairwise correlations and susceptibilities, but their dependence on the temperature, carrier concentration, and model parameters have been investigated. The results obtained for the single-band, two-dimensional Hubbard model with repulsive interaction,⁴¹ for the $t-J$ model,¹⁷ and for the Emery model⁴²⁻⁴⁵ indicate the possibility of s^* - and $d_{x^2-y^2}$ -wave superconductivity.

Therefore, a comprehensive study of the effects of size on pairwise correlations is necessary to settle the question of s^* - and d -symmetry in the thermodynamic limit for the Emery model. We note however, that the maximum size of a cluster in the CuO_2 plane analyzed using the Monte Carlo simulation is 8×8 CuO_2 cells ($N_a=192$), and scaling data presented by Frick *et al.*²⁷ are based on an analysis of only two clusters, consisting of 4×4 and 8×8 cells. Most of the data on coupling symmetry were derived from an analysis of 4×4 and 6×6 clusters ($N_a=48$ and 108 , respectively).⁴² The real correlation lengths are comparable to the linear size of these clusters.²⁶

Unfortunately, the convergence time of well-known deterministic and variational Monte Carlo algorithms is proportional to N_a^3 , so the use of these algorithms is limited to clusters with $N_a > 200$ atoms.

Elesin and Kashurnikov²⁶ proposed a new path-integral Monte Carlo algorithm for CuO_2 clusters with considerably faster convergence (the convergence time is proportional to N_a), which is, to the best of our knowledge, the first path-integral technique for two-dimensional fermion systems. It was used to calculate energy parameters of Cu-O clusters with $N_a=12, 24, 30, \dots, 108$ atoms, and to obtain the energies, occupation numbers, and other parameters as functions of the cluster size.²⁶ But given well-known limitations of path-integral Monte Carlo algorithms, such as the inability to calculate thermodynamic averages of operators that do not conserve the number of particles in a CuO_2 unit cell, this technique cannot be used to investigate pairwise correlation functions, which are highly nonlocal parameters. In addition, the configurations studied in Ref. 26 are anisotropic, which does not matter in calculations of local characteristics, but precludes the analysis of symmetry properties.

This paper proposes a new quantum path-integral Monte Carlo algorithm in which the plane is divided not into three-atom CuO_2 cells,²⁶ but into more symmetrical five-atom CuO_4 cells. In addition, temporal cross sections cutting fermion paths in configuration space are introduced to investigate nonlocal pairwise correlations, and all information is taken from these cross sections. As a result, the CPU time increases somewhat, but it is still proportional to N_a .

The technique has been used to calculate pairwise correlations due to s^- , s^* , and $d_{x^2-y^2}$ -wave coupling for a set of two-dimensional clusters with $N_a=48, 108, 192, 300, 432, 588, \text{ and } 768$ atoms, the largest cluster studied (16×16 CuO_2 cells) being four times the largest system investigated by existing Monte Carlo techniques. Given this set of clusters, the plausibility of various superconductive coupling modes has been properly analyzed, and it has turned out that in the temperature range studied ($T \sim 0.1t$, where $t \approx 1$ eV) pairwise correlations tend to a constant as $N_a \rightarrow \infty$, rather than diverging, i.e., the lack of superconducting correlations in the thermodynamic limit is evident.

Nonetheless, the matter is not settled yet because at lower temperatures the amplitudes of pairwise correlations are larger (as follows from our calculations), ferromagnetic ordering occurs, and the behavior of correlations at a temperature close to that of the phase transition is hard to predict.

2. EMERY MODEL AND PAIRWISE CORRELATION FUNCTIONS

Consider the two-dimensional, multiband Emery model for a CuO_2 plane,²⁰ which takes into account the hybridization of copper $d_{x^2-y^2}$ and oxygen p_x, p_y orbitals, the mismatch between atomic levels at copper and oxygen lattice sites, and Coulomb interaction at copper and oxygen sites and between them.

In the hole representation, the Emery Hamiltonian is

$$H = -t \sum_{\langle ik \rangle, \sigma} (d_{i\sigma}^+ p_{k\sigma} + \text{h.c.}) + \varepsilon \sum_{k, \sigma} n_{k\sigma} + U_d \sum_i n_{i\uparrow} n_{i\downarrow} + U_p \sum_k n_{k\uparrow} n_{k\downarrow} + V \sum_{\langle ik \rangle, \sigma, \sigma'} n_{i\sigma} n_{k\sigma'}, \quad (1)$$

where $d_{i\sigma}^+$ and $p_{k\sigma}^+$ are hole creation operators in $d_{x^2-y^2}$ and p_x, p_y states, respectively; i denotes copper sites; k denotes oxygen sites; $n_{i\sigma} = d_{i\sigma}^+ d_{i\sigma}$, $n_{k\sigma} = p_{k\sigma}^+ p_{k\sigma}$; t is the copper-to-oxygen hopping matrix element; ε is the hole energy difference between oxygen and copper sites; U_d , U_p , and V are the energies of Coulomb repulsion between holes at copper and oxygen sites, and between holes at different sites. The dielectric (undoped) state corresponds to half-filled copper sites (the number of holes, $\langle N \rangle$, is equal to the number of copper sites, N_{Cu}). A higher (lower) number of holes corresponds to the hole (electron) doping of the CuO_2 plane in a high- T_c superconductor.

The relative concentration of carriers (per one CuO_2 elementary cell), $x = \langle N \rangle / N_{\text{Cu}}$, is optimal in terms of T_c over the following ranges: in p -type HTS $x = 1.1 - 1.25$,^{1,46} in

n -doped HTS $x=0.83-0.88$.^{1,47} In this paper we limit our investigation of symmetry properties of pairwise correlation functions to these ranges.

Let us define pairwise correlations as functions of the distance:^{39,42}

$$P_\alpha(\mathbf{r}) = \sum_{\mathbf{l}} \langle \Delta_\alpha(\mathbf{l}) \Delta_\alpha^+(\mathbf{l} + \mathbf{r}) \rangle, \quad (2)$$

where

$$\Delta_\alpha^+(\mathbf{r}) = \frac{1}{\sqrt{N_{\text{Cu}}}} \sum_{\nu} g_\alpha(\nu) C_{r\uparrow}^+ C_{r+\nu\uparrow}^+. \quad (3)$$

The sum in Eq. (2) is performed over all elementary cells of the CuO_2 plane. This means that the operators $C_{r\sigma}^+$ act at equivalent sites, i.e., either at copper atoms with the coordinate \mathbf{R}_{Cu} or at oxygen sites with coordinates $\mathbf{R}_{\text{Cu}} + (a/2)\mathbf{i}$, $\mathbf{R}_{\text{Cu}} + (a/2)\mathbf{j}$, where a is the lattice constant. In accordance with nuclear magnetic resonance (NMR) data,⁴⁸ we select copper atoms as equivalent sites because the pair wave function at these sites has a smaller amplitude than at oxygen sites (nonetheless, Dopf *et al.*⁴⁴ selected $C_{r\uparrow}^+$ at $\mathbf{r} = \mathbf{R}_{\text{Cu}}$, and $C_{r+\nu\uparrow}^+$ at $\mathbf{r} + \nu = \mathbf{R}_{\text{Cu}} + (a/2)\mathbf{i}$ or $\mathbf{r} + \nu = \mathbf{R}_{\text{Cu}} + (a/2)\mathbf{j}$ in their study of coupling within a CuO_2 cell, i.e., so-called Zhang-Rice singlets⁴⁹). Another reason for studying pairwise correlations in this copper sublattice is that the data on carrier attraction in small Cu-O clusters²⁸⁻³⁵ demonstrated the importance of antiferromagnetic fluctuations at copper atoms in coupling of holes. Other theoretical approaches (such as the spin bag model, $t-J$ model, etc., see Ref. 1 and references therein) are largely equivalent to accurately taking into account antiferromagnetism of copper atoms and effectively including the oxygen subsystem through conversion of the Emery model to the simple two-dimensional Hubbard model with respect to the parameters t/ε and t/U_p .

The function $g_\alpha(\nu)$ depends on the coupling mode. At $\alpha = s$ we have $g_\alpha(\nu) = \delta_{\nu,0}$. At $\alpha = s^*$ we have $g_\alpha(\nu) = 1$ for $\nu = \pm a\mathbf{i}$, $\pm a\mathbf{j}$ and $g_\alpha(\nu) = 0$ for other values of ν . When $\alpha = d_{x^2-y^2}$ we have $g_\alpha(\nu) = 1$ at $\nu = \pm a\mathbf{i}$, $g_\alpha(\nu) = -1$ at $\nu = \pm a\mathbf{j}$, and $g_\alpha(\nu) = 0$ for other values of ν . The Fourier component

$$P_\alpha(\mathbf{k}) = \sum_{\mathbf{r}} P_\alpha(\mathbf{r}) \exp(i\mathbf{k}\mathbf{r}) \quad (4)$$

must diverge in the thermodynamic limit at $\mathbf{k} = (0,0)$ if there is off-diagonal long-range order.⁴² Hence the function $P_\alpha(\mathbf{r})$ must drop more and more slowly with distance \mathbf{r} as N_a increases and tend to a constant, which would indicate long-range order.

It is convenient to introduce the following function:^{39,42}

$$\bar{P}_\alpha(\mathbf{k}) = \sum_{\mathbf{r}} \bar{P}_\alpha(\mathbf{r}) \exp(i\mathbf{k}\mathbf{r}), \quad (5)$$

where

$$\begin{aligned} \bar{P}_\alpha(\mathbf{r}) = & \frac{1}{N_{\text{Cu}}} \sum_{\mathbf{l}} \sum_{\nu\nu'} g_\alpha(\nu) g_\alpha(\nu') G_{\uparrow}(\mathbf{l} + \mathbf{r} + \nu, \mathbf{l} \\ & + \nu') G_{\uparrow}(\mathbf{l} + \mathbf{r}, \mathbf{l}) \end{aligned} \quad (6)$$

and $G_\alpha(\mathbf{l}, \mathbf{l}') = \langle C_{\mathbf{l},\sigma} C_{\mathbf{l}',\sigma}^+ \rangle$. Equation (5) is derived from Eq. (2) after decomposition according to Wick's theorem without taking into account anomalous averages $\langle C_{\uparrow}^+ C_{\uparrow}^+ \rangle$ and $\langle C_{\downarrow} C_{\downarrow} \rangle$. In the thermodynamic limit, the right-hand side in Eq. (6) tends to a constant determined by the correlation length, therefore, in the analysis of off-diagonal long-range order at $N_a \rightarrow \infty$, its contribution can be neglected. Note, however, that in a finite cluster this is an essential parameter, so in a proper analysis it is usually subtracted from the right-hand side of Eq. (2).³⁹

The criterion for pairwise correlations due to α -wave coupling in a finite cluster is then as follows:³⁹ if $P_\alpha > \bar{P}_\alpha$, pairwise correlations are generated by α -wave coupling, otherwise there are no pairwise correlations.

We stress that in a calculation with a fixed number of particles and spin component S_z , only anomalous averages like those in Eq. (5) are retained in the pairwise correlation functioning of Eq. (2), hence antiferromagnetic correlations like $\langle C_{\uparrow} C_{\uparrow}^+ \rangle$ and $\langle C_{\downarrow} C_{\downarrow}^+ \rangle$ have no effect. In standard Monte Carlo algorithms⁴⁰⁻⁴⁵ their contribution is always included because a large canonical ensemble is involved.

We select for our numerical calculation only clusters with the symmetry of the CuO_2 plane, and from all possible clusters²⁶ with square symmetry we select only the ones whose basis vectors are parallel to those of the infinite plane. An additional selection criterion is that the number of copper sites must be even (so that the spin component S_z is zero in the undoped state). As a result, we have a set of seven clusters: 4×4 CuO_2 cells ($N_a = 48$), 6×6 (108), 8×8 (192), 10×10 (300), 12×12 (432), 14×14 (588), and 16×16 (768), which allows us to investigate pairwise correlations as functions of the cluster dimension, N_a . The cluster with $N_a = 12$ (2×2 CuO_2 cells) has been already investigated by the exact diagonalization method.³⁶ Furthermore, its symmetry is higher than that of the infinite plane, and it is not included in our set because of its small size.

Let us estimate the typical cluster size sufficient to approach the thermodynamic limit using the data on the correlation length. Experimental data and numerical calculations²⁶ yield a correlation length, ξ , of about 3-4 lattice constants. We can introduce a maximum inequivalent length, L_{max} , equal to $L/2$ for a square cluster with a linear dimension L and periodic boundary conditions. It is reasonable to estimate the thermodynamic limit based on cluster size when $L_{\text{max}} \gg \xi$. Thus the critical clusters in our set are those with $N_a = 108$ and $N_a = 192$, i.e., the largest clusters previously analyzed using the Monte Carlo method.^{27,42}

In our subsequent analysis we calculate pairwise correlations for this set of clusters at various filling factors, selecting the total spin projection $S_z = 0$ in order to minimize the energy and to compensate for finite-size effects.

3. NONLOCAL PATH-INTEGRAL MONTE CARLO TECHNIQUE FOR CuO_2 PLANE

a) Decomposition of the spacetime grid

The Hamiltonian is divided into two parts including bonds of different types:²⁶

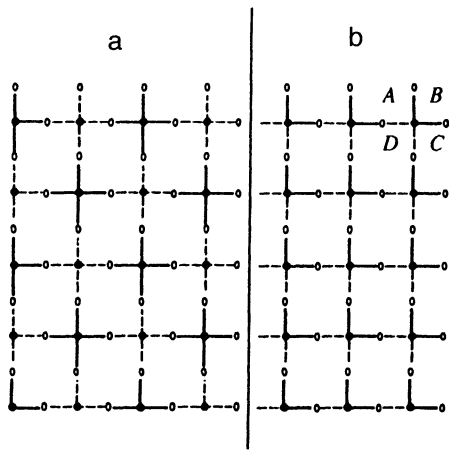


FIG. 1. (a) Decomposition of the CuO₂ plane into two types of bonds for the path-integral Monte Carlo simulation (bonds of type 1 are shown by solid lines, of type 2 by dashed lines). ○ denotes oxygen atoms, ● copper atoms. (b) Decomposition of plane from Ref. 26. One can see that orthogonal directions in the first diagram are equivalent, and in the second diagram the directions A–C and B–D are not.

$$H = H_1 + H_2, \quad H_1 = \sum_{\langle ij \rangle_1} H_{ij}, \quad H_2 = \sum_{\langle ij \rangle_2} H_{ij}. \quad (7)$$

In contrast to the scheme of Ref. 26, the lattice is partitioned as shown in Fig. 1(a), i.e., the entire plane is divided into five-atom CuO₄ cells. Figure 1(b) shows the partition used in Ref. 26. One can see that the directions A–C and B–D are not equivalent because in the model of Ref. 26 motion along the B–D axis between oxygen atoms is forbidden. In the proposed scheme all hops are equivalent, because at finite temperature, diagonal O–O hops are possible,²⁶ and in Fig. 1(a) the diagonals are equivalent.

Using the Trotter expansion⁵⁰ and introducing a complete set of functions in each time slice,^{25,26} we present the partition function in the form of a discrete functional integral:

$$Z = \sum_{i_1 \dots i_{2L}} \langle i_1 | \exp(-\Delta\tau H_1) | i_2 \rangle \langle i_2 | \exp(-\Delta\tau H_2) | i_3 \rangle \dots \langle i_{2L-1} | \exp(-\Delta\tau H_1) | i_{2L} \rangle \langle i_{2L} | \exp(-\Delta\tau H_2) | i_1 \rangle, \quad (8)$$

where $\Delta\tau = \beta/L$.

Let us present Eq. (8) in a graphic form. Consider $2L$ identical two-dimensional Cu–O clusters with a number of atoms N_a above one another along the time axis (Fig. 2). The sum in Eq. (8) is taken over all possible closed noncrossing paths. Hops between paths are allowed only on cross-hatched vertical faces. Two filling factors, n_\uparrow and n_\downarrow , equal either to 1 or 0, correspond to each site, therefore the paths (world lines) for each spin projection are decoupled.

Transitions between time slices are determined by matrix elements of the evolution operator

$$U_{n,n+1} = \sum_{K=0}^{\infty} \frac{(-\Delta\tau)^K}{K!} \langle i_n | H_{1,2} | i_{n+1} \rangle^K / K!. \quad (9)$$

The total number of states in a CuO₄ cell is 1024, therefore each evolution operator in Eq. (9) is a 1024×1024 array. The evolution operator is calculated numerically using Eq. (9) with the sum cut off when the required accuracy is achieved.

In this connection, we note two features of this scheme:

1) The probabilities of hops between trajectories on the O–O diagonal, of a virtual O–O transition via a copper site, and of combined transitions $C_{5\uparrow}^+ C_{1\uparrow} C_{5\downarrow}^+ C_{2\downarrow}$,

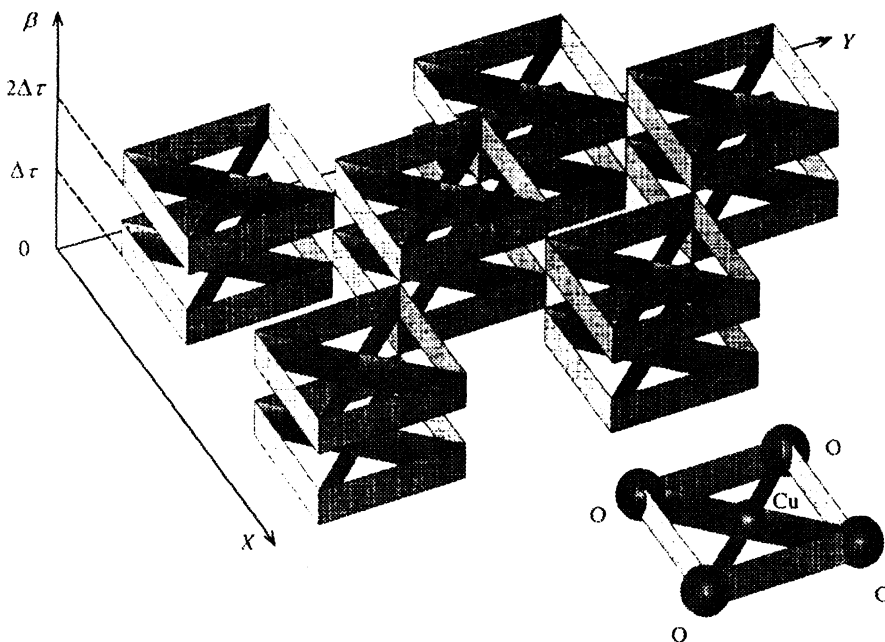


FIG. 2. Spacetime grid for the Monte Carlo simulation. Fermion world lines can only cross on cross-hatched faces.

$C_{5\uparrow}^+ C_{1\uparrow} C_{4\uparrow} C_{2\uparrow}$, etc., are nonzero even to second order in $\Delta\tau$. Therefore these motions of holes should be included in the Monte Carlo scheme.

2) The signs of U_{nn+1} matrix elements in the real Monte Carlo configuration must be known. Simple multiplication of the matrices in Eq. (9), expanded in the five-site cell basis, does not yield this information because the numbering of sites in an isolated cell is different from that in CuO_4 cells in a studied cluster. The following procedure is used for this reason.

First, the $\exp(-\Delta\tau H)$ operator is calculated exactly, i.e., the sum on the right of Eq. (9) is obtained in analytic form. This problem is nontrivial: after enough multiplications, the number of irreducible summands in the Emery Hamiltonian for a five-atom CuO_4 cell ordered with respect to the atom numbers within one cell like $C_{i_1\uparrow}^+ C_{i_1\uparrow} C_{i_2\uparrow}^+ C_{i_2\uparrow} C_{j_1\uparrow}^+ C_{j_1\uparrow} C_{j_2\uparrow}^+ C_{j_2\uparrow} C_{k_1\uparrow}^+ C_{k_1\uparrow} C_{k_2\uparrow}^+ C_{k_2\uparrow} C_{l_1\uparrow}^+ C_{l_1\uparrow} C_{m_1\uparrow}^+ C_{m_1\uparrow} C_{n_1\uparrow}$, etc. (here $i, j, k=1-5$, $i_1 > i_2 > i_3 \dots, j_1 > j_2 > j_3 \dots, k_1 > k_2 > k_3 > \dots, l_1 > l_2 > l_3 > \dots$, and all indices i, j, k are different) in Eq. (9) is up to its maximum of 63504. Nonetheless, this problem can be solved on a computer. Then we apply the resulting operator to the wave function to derive U_{nn+1} and information on its sign.

The subsequent procedure is similar to that used in Refs. 25 and 26, namely interchanging configurations via the Metropolis algorithm⁵¹ and calculating the ratio of products of evolution matrix elements before and after the interchange.

b) Thermodynamic averages of physical parameters, nonlocal effects

Thermodynamic averages of operators that conserve the number of particles in a CuO_4 cell are calculated similarly to familiar path-integral Monte Carlo algorithms,^{25,26} so we shall not dwell on this matter.

Pairwise correlation functions are nonlocal characteristics, since these operators break fermion world lines and change the number of particles in one cell. In this case, we introduce additional time cross sections between which trajectories may be broken.²⁵ Then the thermodynamic average of such an operator takes the form:

$$\langle Q \rangle = \langle Q_1 \rangle / \langle W_1 \rangle, \quad (10)$$

$$\langle Q_1 \rangle = \text{Tr}[\langle i_1 | Q | i_1' \rangle U_{1',2} U_{2,3} \dots U_{2L,1}], \quad (11)$$

$$\langle W_1 \rangle = \text{Tr}[\langle i_1 | i_1' \rangle U_{1',2} U_{2,3} \dots U_{2L,1}]. \quad (12)$$

In calculations with Eq. (10), the numerator and denominator must be computed via independent Monte Carlo procedures. We have integrated these procedures by adding new terms either to the numerator or denominator, depending on which of the matrix elements, $\langle i_1 | Q | i_1' \rangle$ or $\langle i_1 | i_1' \rangle$, is nonzero. All useful information is removed from the $\langle i_1 | i_1' \rangle$ cross section, and as a result, the convergence rate is reduced by a factor of $2L$, but the total CPU time is nonetheless linear with respect to the number of atoms, N_a , in a cluster.

In order to achieve the required accuracy, we perform about 10^3 Monte Carlo steps to thermalize the system and

about 10^4 steps to calculate averages. The statistical uncertainties are estimated using the proper procedure²⁶ and are within several percent.

The uncertainty of the statistical weight sign (minus-sign problem) does not significantly affect the convergence of this algorithm because it tends to a constant at $T \rightarrow 0$.

The algorithm has been tested by calculating characteristics of a twelve-atom Cu_4O_8 cluster using exact diagonalization,³⁶ and of other clusters using both deterministic and variational Monte Carlo techniques,^{27,42} leading us to the following conclusions:

1) For a p -doped Cu_4O_8 cluster ($\langle N \rangle = 5$) at $U_d = 6$, $\varepsilon = 1$, and $T = 0.125$ we have $P_d - \overline{P}_d = 0.02$, $P_{s^*} - \overline{P}_{s^*} = 0.03$, while the exact diagonalization technique at $T = 0$ yields³⁶ $P_d - \overline{P}_d = 0.05$, $P_{s^*} - \overline{P}_{s^*} = 0.1$, i.e., the temperature reduces pairwise correlations, as expected, by a factor of more than two, and the ratios of amplitudes in s^* and d -modes are changed little.

2) The results are identical, within the calculation uncertainty, to those of standard Monte Carlo algorithms^{27,42} for clusters with $N_a = 48, 108$, and 192 after some modifications because pairwise correlations like $\langle \Delta^+ \Delta \rangle$ are often calculated instead of those in Eq. (2).

4. PAIRWISE CORRELATION FUNCTIONS

Pairwise correlations for Cu-O clusters in the Emery model have been calculated at the following Hamiltonian parameters in Eq. (1): $\varepsilon = 1-3$, $U_d = 6$, $U_p = V = 0$ (in units of t). These values were selected because, first, they are typical figures derived from experimental data^{52,53} and, second, basic results concerning binding energy and pairwise correlations using the exact diagonalization method in the Cu_4O_8 cluster,²⁸⁻³⁶ and the symmetry of coupling in clusters with $N_a = 48, 108$, and 192 ⁴²⁻⁴⁵ using the Monte Carlo method were obtained in this range of parameters.

Let us first consider the parameter $P_\alpha \equiv P_\alpha(k)$ at $k = (0,0)$ as a function of the cluster size at $\alpha = s, s^*$, and $d_{x^2-y^2}$. Figure 3 shows calculations of $\chi_\alpha = \sqrt{P_\alpha / N_{\text{Cu}}}$ versus $\sqrt{1/N_{\text{Cu}}}$ for p -doped clusters with $N_a = 48, 108, \dots, 768$ at $x = 1.125$ and $x = 1.25$ by the path-integral Monte Carlo technique. These data indicate that the parameter P_α does not diverge with increasing N_a , but on the contrary, tends to a constant for all coupling modes. This result is in agreement with data from Ref. 27 on s -wave coupling in clusters with $N_a \leq 192$ and suggests a lack of off-diagonal long-range order in the thermodynamic limit, i.e., at finite temperature.

This conclusion is supported by other calculations. Figure 4 shows $P_\alpha(\mathbf{r})$ versus the coordination sphere number in the copper sublattice. In fact, $P_\alpha(\mathbf{r})$ drops to zero within two or three coordination spheres (approximately two lattice constants) for all cluster sizes considered in this paper, which is confirmed by a lack of long-range order effects. Similar behavior of P_α was observed in the two-dimensional Hubbard model³⁸ at $\alpha = s$. Note that a cluster with $N_a = 300$ is sufficient to approximate the thermodynamic limit, as was suggested by the correlation length evaluation, so that parameters of large clusters ($N_a = 432, 588$, and 768) are essentially equal to within the numerical errors.

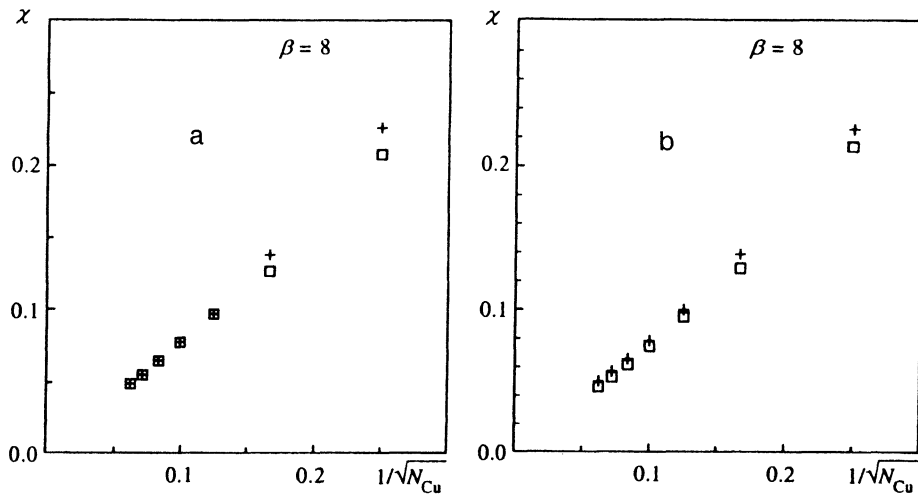


FIG. 3. Parameter $\chi = \sqrt{P_\alpha/N_{Cu}}$ plotted against $\sqrt{1/N_{Cu}}$ for clusters with $N_a=48, 108, \dots, 768$ at doping levels $x=1.125$ (+) and $x=1.25$ (\square), $\epsilon=1$, $U_d=6$: a) $\alpha=s$; b) $\alpha=s^*$ (in the case of $\alpha = d_{x^2-y^2}$ the results are essentially identical to those for $\alpha=s^*$). For Hamiltonian parameters $\epsilon=3$ and $U_d=6$ and a doping of $x=1.25$ the results are essentially identical to those for the case $\epsilon=1$, $U_d=6$, and $x=1.125$ (+) for all coupling modes.

Since the temperature in the model is high (relative to the critical temperature), the absence or presence of pairwise correlations at $T \rightarrow T_c$ remains an open question. In order to elucidate the problem, it is useful to consider the temperature dependence of $P_\alpha - \overline{P}_\alpha$ (\overline{P}_α is subtracted in order to limit finite-size effects and antiferromagnetic ordering effects for an actual cluster). Figure 5, in which $P_\alpha - \overline{P}_\alpha$ is plotted versus temperature at $N_a=300$ and $x=1.125$, demonstrates that the correlations rise sharply as the temperature decreases. In order to find out whether there is a tendency toward off-diagonal long-range order, the function $P_\alpha(\mathbf{r}) - \overline{P}_\alpha(\mathbf{r})$ is plotted for different temperatures (Fig. 6). As the temperature decreases, the spatial distribution clearly displays antiferro-

magnetic behavior while maintaining a constant correlation length.

The rise in antiferromagnetic correlations in pairwise interactions is explicitly demonstrated by the temperature dependence of $P_\alpha(k) - \overline{P}_\alpha(k)$ at $k=(\pi, \pi)$ (Fig. 7), since at a momentum of (π, π) the antiferromagnetic contribution to the correlator $\langle \Delta \Delta^+ \rangle$ is maximum. An appreciable increase in correlation (for the s^* -coupling it increases by a factor of about five over the temperature range from $T=0.25$ to $T=0.125$) indicates that the main contributor to pairwise correlation is antiferromagnetic ordering. Furthermore, it is interesting to note that a typical correlation scale length is about six coordination spheres (i.e., three lattice constants),

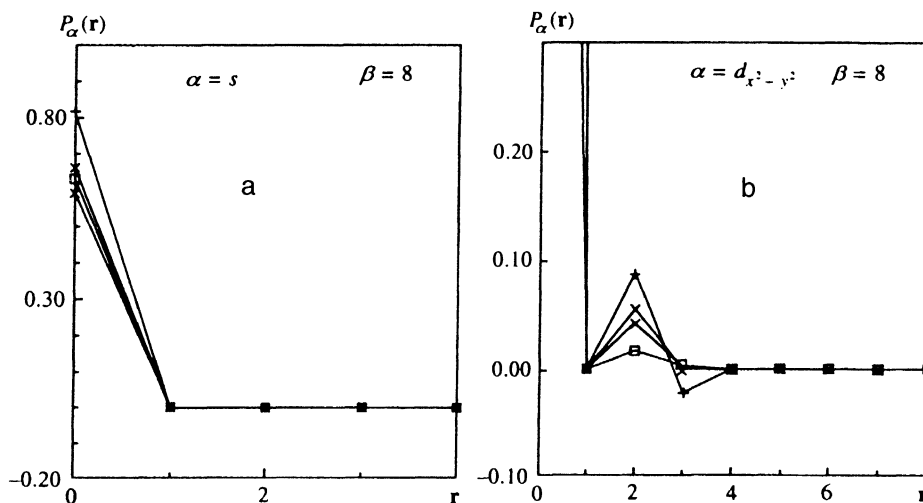


FIG. 4. Correlation $P_\alpha(\mathbf{r})$ as a function of the coordination sphere number in the copper sublattice at a doping $x=1.125$ and cluster dimensions $N_a=48$ (+); 108 (*); 192 (\square); 300 (\times): a) $\alpha=s$; b) $\alpha = d_{x^2-y^2}$ (at $\alpha=s^*$ the spatial distribution also drops within two or three coordination spheres), $\epsilon=1$, $U_d=6$. For clusters with $N_a=432, 588$, and 768 the distribution function coincides within the calculation uncertainty with the data for $N_a=300$.

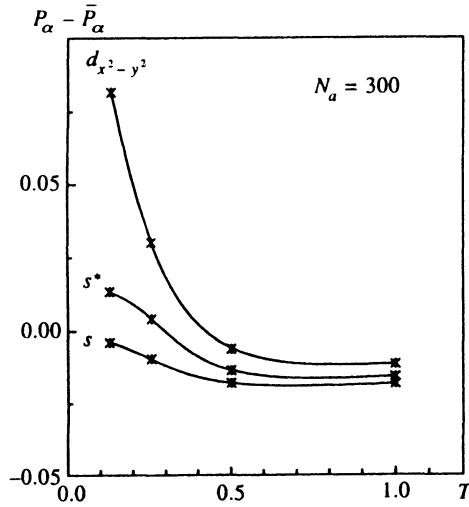


FIG. 5. Temperature dependence of $P_\alpha - \bar{P}_\alpha$ at a doping level $x=1.125$ for a cluster with $N_a=300$ and s -, s^* -, and $d_{x^2-y^2}$ -wave coupling, $\varepsilon=1$, $U_d=6$.

which coincides with the previous antiferromagnetic length calculation.²⁶ The temperature in our calculations is close to that of the antiferromagnetic transition ($T \sim 1000$ K), so it is quite natural that fluctuations related to this transition are displayed by the curves.

To conclude this section, note that calculations were carried out at carrier concentrations of $0.7 \leq x \leq 1.5$, i.e., they include both electron and hole doping. The results for n -doped states are essentially identical to those reported in the present section, i.e., no coupling mode leads to superconductivity, since P_α tends to a constant as the cluster size increases, and the function $P_\alpha(r)$ drops over a distance of two to three lattice constants. The function $P_\alpha - \bar{P}_\alpha$ peaks at half-full copper sites ($x=1.0$), and the range of positive val-

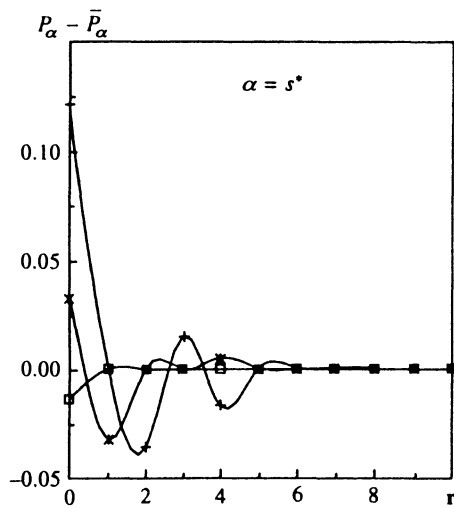


FIG. 6. Spatial distribution of $P_\alpha(r) - \bar{P}_\alpha(r)$ at $N_a=300$ and $\alpha=s^*$, $T=0.125$ (+), 0.25 (*), 0.5 (□), $\varepsilon=1$, $U_d=6$. Antiferromagnetic ordering, which occurs as the temperature falls, decreases with a typical scale length of four to six coordination spheres. The results for $\alpha = d_{x^2-y^2}$ -coupling are qualitatively similar.

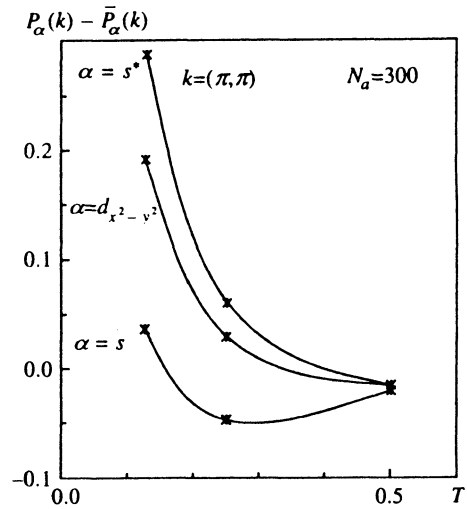


FIG. 7. $P_\alpha(k) - \bar{P}_\alpha(k)$ at $k=(\pi, \pi)$ versus temperature for a cluster with $N_a=300$ for s -, s^* - and $d_{x^2-y^2}$ -coupling. s^* -wave coupling is apparently most susceptible to antiferromagnetic interaction.

ues corresponds to $x=0.8-1.0$ for electron doping and to $x=1.0-1.5$ for hole doping. Antiferromagnetic ordering is actually observed when the concentrations are about equal,¹ and antiferromagnetic effects should be strongest in the undoped ($x=1.0$) state.

5. CONCLUSIONS

This paper proposes a new nonlocal two-dimensional path-integral quantum Monte Carlo technique based on a rapidly convergent decomposition of the CuO_2 plane into five-atom CuO_4 cells. Pairwise correlation functions are calculated by including in the Monte Carlo scheme additional time slices breaking fermion world lines. The first Monte Carlo simulation of a two-dimensional Cu-O cluster with $N_a=768$ atoms (16×16 CuO_2 cells) is reported.

The calculation of pairwise correlation functions due to s , s^* , and $d_{x^2-y^2}$ coupling modes leads to the following conclusions.

In the range of Emery Hamiltonian parameters considered ($U_d=6t$, $\varepsilon=1-3t$, $U_p=V=0$), temperature ($T \geq 0.125t$), and carrier concentration ($0.7 \leq c \leq 1.5$)

a) no off-diagonal long-range order is detected in the thermodynamic limit for all coupling modes;

b) there is a tendency to divergence in the s^* and $d_{x^2-y^2}$ modes with decreasing temperature, but the analysis indicates that the main contributor to this effect is antiferromagnetic ordering. Furthermore, the typical scale length of the correlation function is close to the typical antiferromagnetic length calculated previously.²⁶

We stress that the possibility of superconducting coupling should be investigated by scaling system parameters at a temperature close to T_c . In principle, the superconducting state can be identified using other criteria not including the wave function symmetry. For example, Assaad *et al.*⁵⁴ derive the density of superconducting pairs from the ground state energy as a function of the phase Φ . In particular, they did

not detect the superconducting component in the Emery model even at a record low (for Monte Carlo simulations) temperature $T=1/16t$.

I am grateful to V. F. Elesin, L. A. Openov, A. V. Krasheninnikov, and E. V. Kholmovskii for helpful discussions and valuable remarks, which were taken into account in writing the paper.

This work was supported by the International Science Foundation, Grant No. M67300, and the Scientific Counsel on the High- T_c Superconductivity Problem (project No. 94031 in the High-Temperature Superconductivity Program).

- ¹E. Dagotto, *Rev. Mod. Phys.* **66**, 763 (1994); D. J. Scalapino, *Phys. Rep.* **250**, 329 (1995).
- ²V. J. Emery, *Nature* **370**, 598 (1994).
- ³P. Mountoux and D. Pines, *Nuovo Cimento D* **15**, 181 (1993).
- ⁴S. Chakraverty, A. Sudbo, P. W. Anderson and S. Strong, *Science* **261**, 337 (1993).
- ⁵J. R. Schrieffer, X. G. Wen, and S. C. Zhang, *Phys. Rev. B* **39**, 11663 (1989).
- ⁶J. R. Kirtley, C. C. Truel, J. Z. Sun *et al.*, *Nature* **373**, 225 (1995).
- ⁷I. Iguchi and Z. Wen, *Phys. Rev. B* **49**, 12388 (1994).
- ⁸A. G. Sun, D. A. Gajewski, M. B. Maple, and R. C. Dynes, *Phys. Rev. Lett.* **72**, 2267 (1994).
- ⁹C. C. Tsuei, J. R. Kirtley, C. C. Chi *et al.*, *Phys. Rev. Lett.* **73**, 593 (1994).
- ¹⁰D. A. Wollman, D. J. Van Harlingen, W. C. Lee *et al.*, *Phys. Rev. Lett.* **71**, 2134 (1993).
- ¹¹J. Buan, Branko P. Stojkovic, N. E. Israeloff *et al.*, *Phys. Rev. Lett.* **72**, 2632 (1994).
- ¹²M. Bankay, M. Mali, J. Roos, and D. Brinkmann, *Phys. Rev. B* **50**, 6416 (1994).
- ¹³T. P. Devereaux, D. Einzel, B. Stadlober *et al.*, *Phys. Rev. Lett.* **72**, 396 (1994).
- ¹⁴J. Kane, Q. Chen, K. W. Ng, and H. J. Tao, *Phys. Rev. Lett.* **72**, 128 (1994).
- ¹⁵Hond Ding, J. G. Campuzano, K. Gofron *et al.*, *Phys. Rev. B* **50**, 1333 (1994).
- ¹⁶P. Chaudhari and Shawn-Yu Lin, *Phys. Rev. Lett.* **72**, 1084 (1994).
- ¹⁷Q. P. Li, B. E. C. Koltenbah, and R. Joynt, *Phys. Rev. B* **48**, 437 (1993); J. E. Sonier, R. F. Kieft, J. H. Brewer *et al.*, *Phys. Rev. Lett.* **72**, 744 (1994).
- ¹⁸R. J. Kelley, J. Ma, G. Margaritondo, and M. Oneilion, *Phys. Rev. Lett.* **71**, 4051 (1993).
- ¹⁹D. C. Mattis, *Mod. Phys. Lett. B* **4**, 1171 (1990); F. C. Zhang and T. M. Rice, *Phys. Rev. B* **37**, 3759 (1988).
- ²⁰V. J. Emery, *Phys. Rev. Lett.* **58**, 2794 (1987).
- ²¹P. B. Littlewood, C. M. Varma, S. Schmidt-Rink, and E. Abrahams, *Phys. Rev. B* **39**, 12371 (1989).
- ²²S. Nimkar, D. D. Sarma, H. R. Krishnamurthy, and S. Ramasesha, *Phys. Rev. B* **48**, 7355 (1993).
- ²³J. E. Hirsch, S. Tang, E. Loh Jr., and D. J. Scalapino, *Phys. Rev. Lett.* **60**, 1668 (1988).
- ²⁴V. F. Elesin, V. A. Kashurnikov, L. A. Openov, and A. I. Podlivaev, *Zh. Éksp. Teor. Fiz.* **99**, 237 (1991) [*JETP* **72**, 133 (1991)].
- ²⁵J. E. Hirsch, R. L. Sugar, D. J. Scalapino, and R. Blankenbecler, *Phys. Rev. B* **26**, 5033 (1982).
- ²⁶V. F. Elesin and V. A. Kashurnikov, *Zh. Éksp. Teor. Fiz.* **106**, 1773 (1994) [*JETP* **79**, 961 (1994)].
- ²⁷M. Frick, P. C. Pattnaik, I. Moraenstern *et al.*, *Phys. Rev. B* **42**, 2665 (1990).
- ²⁸L. Tan, Q. Li, and J. Callaway, *Phys. Rev. B* **44**, 341 (1991).
- ²⁹J. E. Hirsch, E. Loh Jr., D. J. Scalapino, and S. Tang, *Phys. Rev. B* **39**, 243 (1989).
- ³⁰V. F. Elesin, V. A. Kashurnikov, L. A. Openov, and A. I. Podlivaev, *Zh. Éksp. Teor. Fiz.* **101**, 682 (1992) [*JETP* **74**, 363 (1992)].
- ³¹V. F. Elesin, V. A. Kashurnikov, L. A. Openov, and A. I. Podlivaev, *Physica C* **195**, 171 (1992).
- ³²V. F. Elesin, V. A. Kashurnikov, and A. I. Podlivaev, *Zh. Éksp. Teor. Fiz.* **104**, 3835 (1993), [*JETP* **77**, 841 (1993)].
- ³³V. F. Elesin, V. A. Kashurnikov, A. V. Krasheninnikov, and A. I. Podlivaev, *Physica C* **222**, 127 (1994).
- ³⁴V. F. Elesin, V. A. Kashurnikov, A. V. Krasheninnikov, and A. I. Podlivaev, *Zh. Éksp. Teor. Fiz.* **105**, 1759 (1994), [*JETP* **78**, 951 (1994)].
- ³⁵V. F. Elesin, V. A. Kashurnikov, L. A. Openov, and A. I. Podlivaev, *Sol. St. Comm.* **89**, 27 (1994).
- ³⁶V. F. Elesin, A. V. Krasheninnikov, and L. A. Openov, *Zh. Éksp. Teor. Fiz.* **106**, 1459 (1994), [*JETP* **79**, 789 (1994)].
- ³⁷D. Poiblanc, *Phys. Rev. B* **48**, 3368 (1993); E. Dagotto and J. Riera, *Phys. Rev. B* **46**, 12084 (1992).
- ³⁸A. Moreo and D. J. Scalapino, *Phys. Rev. Lett.* **66**, 946 (1991).
- ³⁹A. Moreo, *Phys. Rev. B* **45**, 5059 (1993).
- ⁴⁰R. T. Scalettar, J. W. Cannon, D. J. Scalapino, and R. L. Sugar, *Phys. Rev. B* **50**, 13419 (1994).
- ⁴¹R. E. Hetzel, W. von der Linden, and W. Hanke, *Phys. Rev. B* **50**, 4159 (1994).
- ⁴²R. T. Scalettar, D. J. Scalapino, R. L. Sugar, and S. R. White, *Phys. Rev. B* **44**, 770 (1991).
- ⁴³M. Imada, *J. Phys. Soc. Jpn.* **56**, 3793 (1987); **57**, 3128 (1988).
- ⁴⁴G. Dopf, A. Muramatsu, and W. Hanke, *Phys. Rev. B* **41**, 9264 (1990).
- ⁴⁵A. Bhattacharya and C. S. Wang, *Phys. Rev. B* **48**, 13949 (1993).
- ⁴⁶H. Zang and H. Sato, *Phys. Rev. Lett.* **70**, 1697 (1993).
- ⁴⁷O. G. Singh, B. D. Padalia, O. Prakash *et al.*, *Physica C* **219**, 156 (1994).
- ⁴⁸P. C. Hammel, M. Takigawa, R. H. Heffner *et al.*, *Phys. Rev. Lett.* **63**, 1992 (1989).
- ⁴⁹F. C. Zhang and T. M. Rice, *Phys. Rev. B* **37**, 3759 (1988).
- ⁵⁰M. Suzuki, *Phys. Lett. A* **113**, 299 (1985).
- ⁵¹N. Metropolis, A. W. Rosenbluth, M. N. Rosenbluth *et al.*, *J. Chem. Phys.* **21**, 1087 (1953).
- ⁵²A. K. McMahan, J. F. Annet, and R. M. Martin, *Phys. Rev. B* **42**, 6268 (1990).
- ⁵³H. Rushan, C. K. Chew, K. K. Phua, and Z. Z. Gan, *J. Phys. C* **3**, 8059 (1991).
- ⁵⁴F. F. Assaad, W. Hanke, and D. J. Scalapino, *Phys. Rev. B* **50**, 12835 (1994).

Translation was provided by the Russian Editorial office.